International Journal of Fluid Machinery and Systems
Vol. 4, No. 4, October-December 2011

DOI: http://dx.doi.org/10.5293/IJFMS.2011.4.4.367
ISSN (Online): 1882-9554

Original Paper

Effects of the Geometry of Components Attached to the Drain Valve on the Performance of Water Hammer Pumps

Sumio Saito[1], Masaaki Takahashi[2], Yoshimi Nagata[3], and Keita Dejima[1]

[1]Department of Mechanical Engineering, Tokyo National College of Technology,
1220-2 Kunugida-machi, Hachioji-shi, Tokyo, 193-0997, Japan
[2]Mechanical and Computer Systems Engineering, Advanced Engineering Course,
Tokyo National College of Technology,
1220-2 Kunugida-machi, Hachioji-shi, Tokyo, 193-0997, Japan
[3]Yamaha Motor Engineering Co., Ltd.

Abstract

Water hammer pumps can effectively use the water hammer phenomenon in long-distance pipeline networks that include pumps and allow fluid transport without drive sources, such as electric motors. The results of experiments that examined the effect of the geometric form of water hammer pumps by considering their major dimensions have been reported. In addition, a paper has also been published analyzing the water hammer phenomenon numerically by using the characteristic curve method for comparison with experimental results. However, these conventional studies have not fully evaluated the pump performance in terms of pump head and flow rate, common measures indicating the performance of pumps. Therefore, as a first stage for the understanding of water hammer pump performance in comparison with the characteristics of typical turbo pumps, the previous paper experimentally examined how the hydrodynamic characteristics were affected by the inner diameter ratio of the drive and lifting pipes, the form of the air chamber, and the angle of the drive pipe. To understand the behavior of the components attached to the valve chamber and the air chamber that affects the performance of water hammer pumps, the previous study also determined the relationship between the water hammer pump performance and temporal changes in valve chamber and air chamber pressures according to the air chamber capacity. For the geometry of components attached to the drain valve, which is another major component of water hammer pumps, this study experimentally examines how the water hammer pump performance is affected by the length of the spring and the angle of the drain pipe.

Keywords: Water Hammer Pump, Fluid Transients, Pump Performance, Pressure Fluctuation, Flow Visualization

1. Introduction

Water hammer pumps, which effectively use the water hammer phenomenon that imposes a problem in fluid pipeline networks including pumps, are a promising means for effectively transporting fluid even in regions lacking developed infrastructures due to its ability to transport water without drive sources, such as electric motors.

Conventional studies on water hammer pumps include those that propose configurations mainly for educational purposes [1], [2], [3]; the results of experiments that examined effects of major specifications for the geometric form of water hammer pumps [4], [5]; and a paper that analyzes the water hammer phenomenon numerically by using the characteristic curve method for comparison with experimental results [6]. These studies, however, have not fully evaluated the relationship between pump head and flow rate, common measures indicating pump performance.

With this being the situation, as a first stage for understanding water hammer pump performance in comparison with the characteristics of typical turbo pumps, the previous study [7] experimentally examined how the basic hydrodynamic characteristics are affected by the relationship of the inner diameters of the drive and lift pipes, the form of the air chamber, and the angle of the drive pipe, which are believed to be representative geometric form factors of a water hammer pump. The previous study also clarified the relationship between the temporal pressure fluctuations in the valve and air chambers at different air

Received April 11 2011; revised June 27 2011; accepted for publication September 30 2011: Review conducted by Dr. Hideaki Tamaki. (Paper number O11006J)
Corresponding author: Sumio Saito, Professor, saito@tokyo-ct.ac.jp

volumes in the air chamber and the performance of the water hammer pump, in order to elucidate the flow behavior around the valve and air chambers that affects the characteristics of the water hammer pump system [8].

This study experimentally examines how the length of a spring attached to the drain valve and the drain pipe angle, which are major components of the water hammer pump among other form factors around the drain valve, affect the performance of the water hammer pump.

2. Experimental Apparatus and Method

2.1 Experimental Apparatus

Figure 1 shows an overall schematic diagram of a water hammer pump system, which is the same as the one used in the experiment for the previous study [8]. Figure 2 is a detailed schematic diagram of the water hammer pump, including the valve chamber and its associated parts, illustrating the arrangement of the spring ⑧ attached to the drain valve ④ and the drain pipe ⑨ adjustable at three angles θ_d.

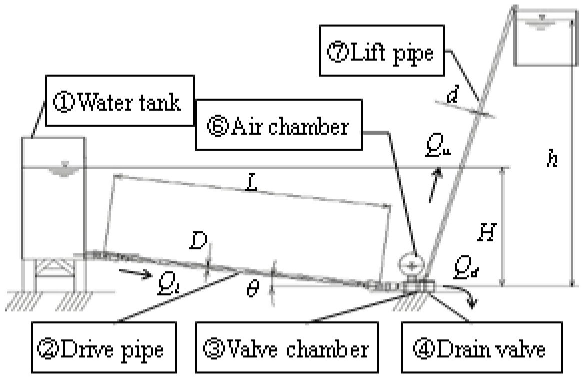

Fig. 1 Water hammer pump system

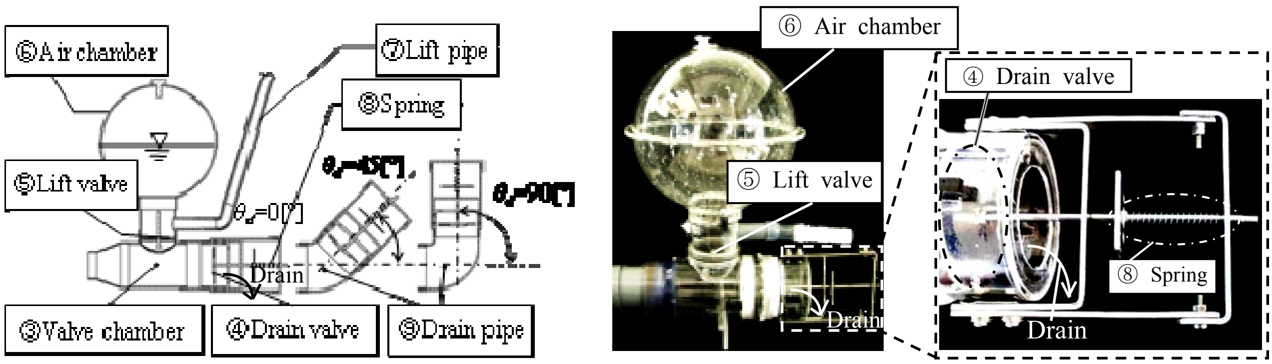

Fig. 2 Main parts of the water hammer pump

The pump is composed of main parts from the water tank ① to the drain pipe ⑨. The drive pipe ②, which supplies water from the water tank ① to the valve chamber ③, is made of acrylic resin to allow observation of internal flow. The valve chamber ③ and the spherical air chamber ⑥ are also made of acrylic resin material and configured such that ink can be injected for visualization of flow in the valve chamber.

The spring ⑧ located downstream of the drain valve ④ acts to bias the drain valve open. For the spring ⑧, springs of three different lengths were used for the experiment: a spring with a length of ℓ_s = 70.0 [mm] (designated as "3/3") as the reference, a spring that is two thirds the reference length (designated as "2/3", ℓ_s= 46.7 [mm]), and a spring that is one third the reference length (designated as "1/3", ℓ_s = 23.3 [mm]). Each of the springs was placed in the drain valve at its defined length. Since the degree of opening of the drain valve depends on the compression action of the spring during operation of the water hammer pump, the opening degree of the drain valve is larger with a larger spring length.

An elbow was attached to the drain valve ④ to make the drain pipe angle θ_d adjustable at three angles, 0[°], 45[°], and 90[°].

Closing of the drain valve ④ located downstream of the valve chamber ③ causes the water hammer phenomenon, which in turn lifts water through nine 6[mm]-diameter holes in the valve seat of the lift valve ⑤.

2.2 Experimental Conditions and Geometric Form Factors

Table 1 shows factors that affect the hydrodynamic characteristics of the water hammer pump.

Among the factors of Table 1, this study experimentally examined the effects of the spring ⑧ located downstream of the drain valve ④ and the angle of the drain pipe ⑨ on the performance of the water hammer pump. As other major specifications of the water hammer pump for the experiment, the inner diameters of the drive and lift pipes were set at D = 25 [mmφ] and d = 18 [mmφ], respectively, while the drive pipe length was set at L = 4 [m] and its angle at θ = 7[°] based on the results of the previous studies [7], [8].

The water level, which is the difference in height between the water level in the water tank ① and the valve chamber ③, was fixed at $H = 0.5$ [m], and the air volume in the air chamber was maintained at $V_a = 1.94$ [ℓ].

Table 1 Experimental factors of the water hammer pump

Geometrical form factor			Experimental condition		
Drive pipe	Inner diameter	D [mmφ]	25		
	Length	L [m]	4		
	Angle	θ [°]	7		
Drain pipe	Angle	θ_d [°]	0, 45, 90		
Lift pipe	Inner diameter	d [mmφ]	18		
Water level		H [m]	0.5		
Air chamber	Capacity	V [ℓ]	3.85 (Spherical type)		
	Air quantity	V_a [ℓ]	1.94		
Spring	Length	ℓ_s [mm]	23.3	46.7	70.0
	Constant	k [N/mm]	0.18	0.09	0.06

The performance of the water hammer pump is indicated in terms of the relationship between the lifted flow rate Q_u and the pump head h, like the performance of typical turbo pumps. The pump efficiency η was determined using the following equation taking into consideration the input and output flow rates of the water hammer pump[7], [8].

$$\eta = \frac{Q_u \times h}{Q_i \times H} = \frac{Q_u}{Q_d + Q_u} \times \frac{h}{H} = \eta_v \times \frac{h}{H} \quad [\%] \qquad (1)$$

2.3 Experimental Method

The input flow rate Q_i into the water hammer pump was determined by measuring the flow rate entering the water tank ① while keeping the water level in the water tank ① constant. In addition, the lift pipe outlet was set so as to obtain the desired pump head, and the outlet flow rate was measured by a gravimetric method to determine the lifted flow rate Q_u. The drain flow rate Q_d from the drain valve was also directly measured by the gravimetric method.

To elucidate the hydrodynamic behavior of the water hammer pump, temporal fluctuations in pressure P_v in the valve chamber ③ shown in Figure 2 was detected using a strain gauge type pressure transducer (PGM-1KG, manufactured by Kyowa Electronic Instruments Co., Ltd.) and measured with an amplifier and an A/D converter.

The behavior of flow in the valve chamber was evaluated by injecting ink upstream of the valve chamber to visualize the internal flow. The flow velocity in the valve chamber was measured using an electro-magnetic velocity meter (VM-801H, manufactured by KENEK Corporation) capable of measuring flow velocity v_x in the flow direction from the drive pipe and flow velocity v_y in the water lifting direction with its sensor located at the center of the valve chamber and that of the lift valve.

3. Experimental Results and Discussion

3.1 Effects of Length of the Spring Attached to the Drain Valve on Water Hammer Pump Performance

3.1.1 Water Hammer Pump Performance Associated with Changes in Spring Length

Figure 3 shows water hammer pump performance for three different spring lengths with the drain pipe angle set at $\theta_d = 0$[°]. As in the case for turbo pump performance, the first quadrant indicates the relationship between the pump head h and the lifted flow rate Q_u in solid lines, and the relationship between the pump efficiency η and the lifted flow rate Q_u in dotted lines. As performance measures specific to the water hammer pump, the second and fourth quadrants indicate the relationship between the pump head h and the number of water hammer occurrences C and the relationship between the drain flow rate Q_d and the lifted flow rate Q_u, respectively.

In the first quadrant, the relationship between the pump head h and lifted flow rate Q_u is represented by downward-sloping curves, as with typical pump performance. The curves are positioned at higher flow rate side at low pump heads as the spring length decreases, but the performance curves for the 2/3- and 1/3-springs are substantially the same. For all of the three lengths, the performance curves are substantially the same at higher pump heads.

The fourth quadrant shows the relationship between the drain flow rate Q_d and the lifted flow rate Q_u. When the longest 3/3-spring is used, the drain flow rate Q_d is highest over the entire range of the lifted flow rate Q_u because the degree of opening of the drain valve is large. The drain flow rate Q_d is a component of the input flow rate and affects the efficiency η and the volumetric efficiency η_v according to the equation (1). Thus, both η and η_v are smallest when the 3/3-spring is used.

When the 2/3- and 1/3-springs are attached, the drain flow rate is lower; overall, the drain flow rate lowers as the spring length decreases.

In the second quadrant, the number of water hammer occurrences C with the 3/3-spring attached is around 30[count/min] for the range of pump head h used in the experiment. The water hammer occurrence C tends to increase as the spring length decreases, being in the range of 40 to 50[count/min] with the 2/3- and 1/3-springs. This can be ascertained also from the fact that the interval of pressure fluctuations in the valve chamber shortens as the spring length decreases, which is indicated by the waveform of temporal fluctuations in pressure shown in Figure 4, as discussed below.

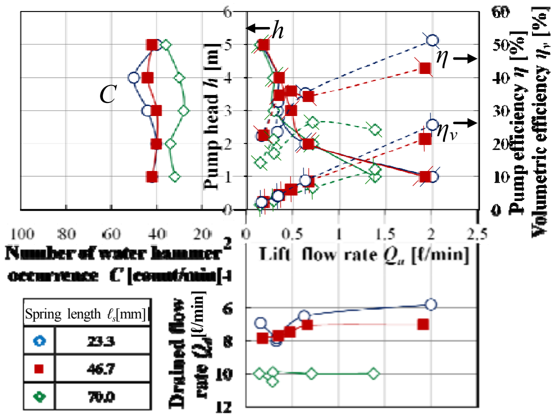

Fig. 3 Change in water hammer pump performance due to spring length (θ_d = 0[°])

3.1.2 Temporal Pressure Fluctuations in the Valve Chamber Associated with Changes in Spring Length and Flow Behavior around the Valve Chamber

Figures 4(a), (b), and (c) show temporal fluctuations in pressure in the valve chamber for three spring lengths with respect to change in the pump head with the drain pipe angle set at θ_d =0[°].

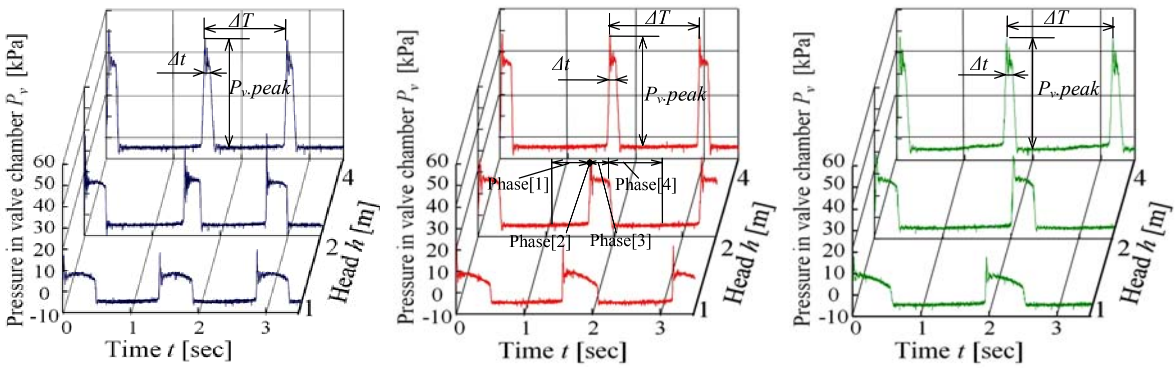

(a) Spring length ℓ_s=23.3[mm] (b) Spring length ℓ_s=46.7 [mm] (c) Spring length ℓ_s=70.0 [mm]

Fig. 4 Pressure fluctuations P_v in valve chamber due to spring length (θ_d= 0[°])

Figure 4(a) shows the result for the 1/3-spring (length ℓ_s =23.3 [mm]). At a high pump head of h =4[m], the waveform of valve chamber pressure is sharper, the peak pressure $P_{v\cdot peak}$ higher, and the pressure holding time during lifting operation Δt shorter. As the pump head lowers, the peak pressure decreases and the pressure holding time during lifting operation Δt increases.

As seen from Figures 4(b) and 4(c), the basic behavior of temporal fluctuations in valve chamber pressure for the longer spring lengths is substantially the same as with the 1/3-spring. Although there are some variations in behavior depending on the pump head, the peak pressure $P_{v\cdot peak}$ slightly decreases while the pressure holding time Δt tends to slightly increase as the spring length increases.

Figure 5 shows visualization of flow in the valve chamber at the pump head of h = 2 [m] with the 2/3-spring (length ℓ_s = 46.7 [mm]) attached and the drain pipe angle set to θ_d= 0[°].

Figure 5 shows photos corresponding to four states from Phase 1 to 4 shown in Figure 6 that represent behavior during the water hammer pump operations [8]. The behavior was observed in increments of 0.1 [sec] for the duration of 1.5 [sec]. Green streaks in the valve chamber are observation ink injected upstream of the valve chamber. By observing the behavior of the ink, qualitative flow fluctuations in the valve chamber during the operations in Phases 1 to 4 shown below can be ascertained. Detailed flow conditions in the valve chamber can be determined from the temporal fluctuations in flow velocity shown in Figure 7 as discussed below.

Phase 1 indicates flow conditions at 0.1[sec], where the drain valve is open and water from the water tank ① flows into the valve chamber.

At 0.7 [sec], which corresponds to Phase 2, the drain valve closes to induce the water hammer phenomenon and the associated pressure causes the lift valve, shown by the single dotted chain line, to start to open.

Phase 3 starts at 0.8 [sec], at which time the lift valve is most open, and goes to 0.9 [sec], at which time the lift valve is just about to close.

At 1.0 [sec], which corresponds to Phase 4, closing of the lift valve and opening of the drain valve occur simultaneously as seen in the photo.

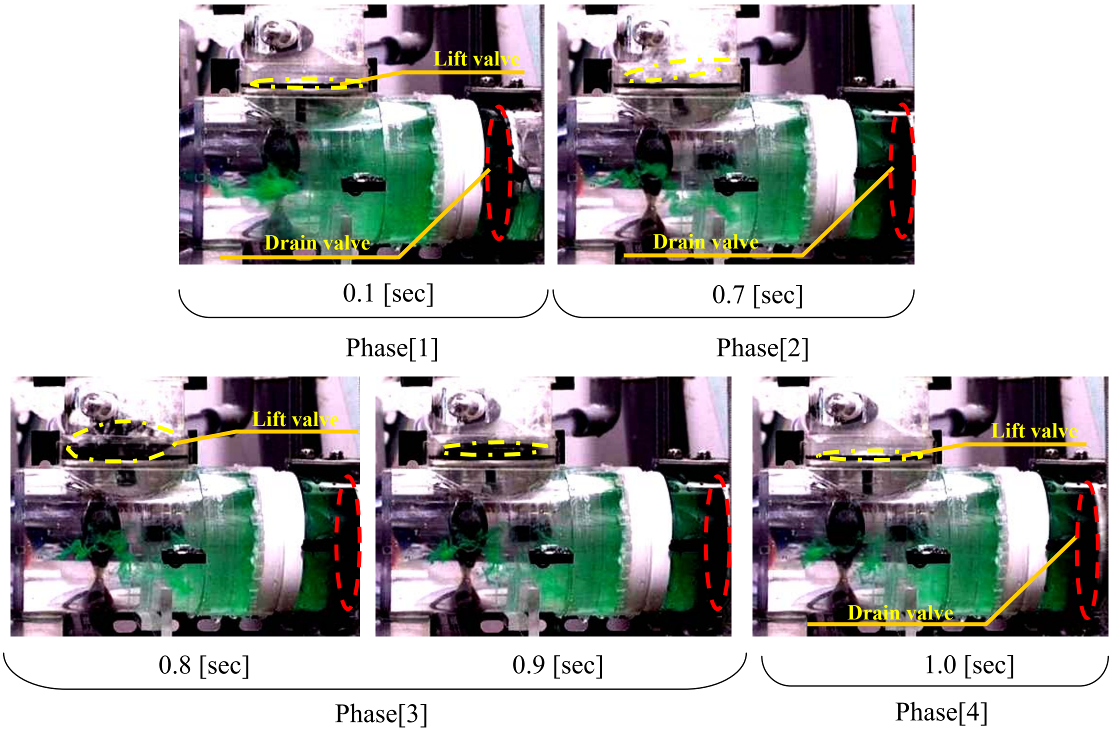

Fig. 5 Flow visualization around valve chamber ($\theta_d = 0$[°], $\ell_s = 46.7$ [mm])

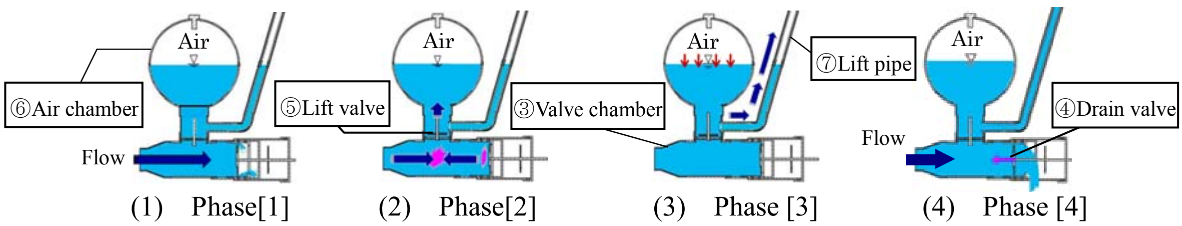

Fig. 6 Water hammer pump operation

Figure 7 shows temporal fluctuations in flow velocities v_x and v_y in the flow and water-lifting directions, respectively, measured at the center of the valve chamber using an electro-magnetic velocity meter under the same conditions as Figure 5.

Combining these observations with the pressure fluctuations in the valve chamber of Figure 4(b) suggests that v_x tends to gradually decrease in Phase 1 and v_y increases with a small delay after Phase 2 at which the drain valve has closed, indicating that water is being lifted. After Phase 3 where the lift valve is open, v_y starts to decrease.

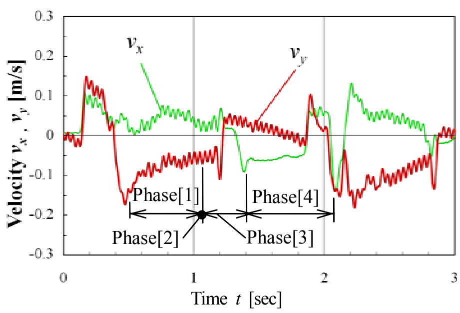

Fig. 7 Velocity fluctuations in valve chamber

3.1.3 Effects of the Length of Spring Attached to the Drain Valve on Pressure Behavior in the Valve Chamber

Based on the results presented above, Figures 8 and 9 show effects of the length of the spring attached to the drain valve on the peak pressure $P_{v\cdot peak}$ of the valve chamber pressure P_v and the pressure holding time during lifting operation Δt at each pump head.

In Figure 8, the peak of the valve chamber pressure P_v is higher at higher pump heads. At lower pump heads, although the pattern of fluctuation for the spring length ℓ_s = 46.7 [mm] is somewhat different from other lengths, spring length has a significant effect on fluctuations in peak pressure $P_{v\cdot peak}$.

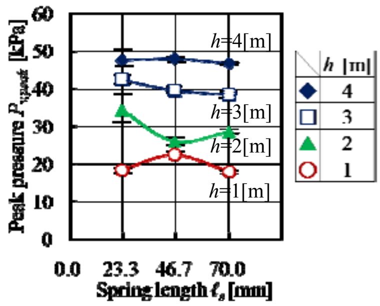

Fig. 8 Relationship between peak pressure $P_{v.peak}$ in valve chamber and spring length

In Figure 9, the pressure holding time during lifting operation Δt in the valve chamber is longer at smaller pump heads. Time Δt tends to slightly increase as spring length increases and rapidly decreases as the pump head increases.

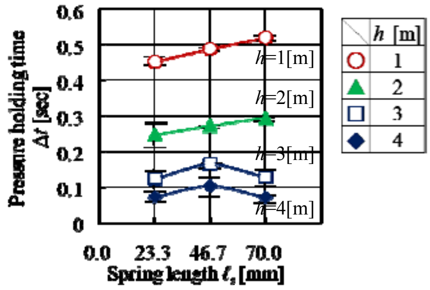

Fig. 9 Relationship between pressure holding time Δt in valve chamber and spring length

3.2 Effects of Drain Pipe Angle on Water Hammer Pump Performance

3.2.1 Water Hammer Pump Performance Associated with Changes in Drain Pipe Angle

Figure 10 shows water hammer pump performance for three drain-pipe angles θ_d, 0[°], 45[°] and 90[°], with the 2/3-spring (ℓ_s = 46.7 [mm]) attached to the drain valve. As with the indication in Figure 3, the first quadrant shows the relationship between pump head h and the lifted flow rate Q_u in solid lines, and relationship between the efficiency η and lifted flow rate Q_u in dotted lines. The second quadrant shows the relationship between the pump head h and the number of water hammer occurrences C, and the fourth quadrant shows the relationship between drain flow rate Q_d and lifted flow rate Q_u.

At the drain pipe angle θ_d = 0[°], pump head h is measured up to around the lifted flow rate of Q_u = 2 [ℓ/min], and the number of water hammer occurrences in the second quadrant is around 40 [count/min] for all the values of pump head. The efficiency for 0[°] is highest as the drain flow rate in the fourth quadrant is lowest across a wide range of the lifted flow rate.

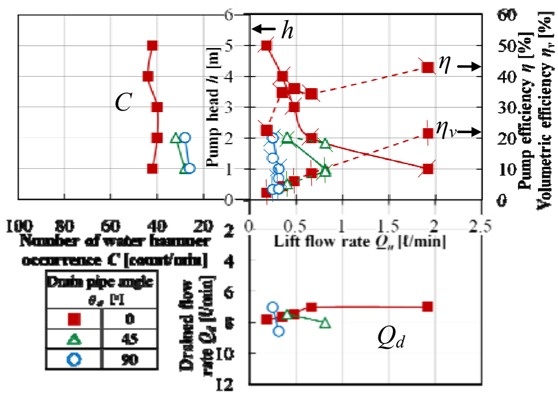

Fig. 10 Change in water hammer pump performance due to drain pipe angle (ℓ_s = 46.7 [mm])

When θ_d= 45[°] and 90[°], the relationship between lifted flow rate and the pump head represents extremely narrow ranges of pump performance compared to when θ_d= 0[°]. The drain valve takes longer to close probably because of the gravity acting in the opening direction of the drain valve caused by the increased drain pipe angle. Hence, the drain flow rate increases and the number of water hammer occurrences shown in the second quadrant decreases to around 30 [count/min] compared to when θ_d= 0[°].

3.2.2 Temporal Pressure Fluctuations in the Valve Chamber Associated with Drain Pipe Angle

Figure 11 shows temporal fluctuations in pressure in the valve chamber when pump head is h = 2[m] for three drain pipe angles θ_d, 0[°], 45[°] and 90[°], with the 2/3-spring (ℓ_s = 46.7 [mm]) attached to the drain valve. Figure 12 shows the interval ΔT of pressure fluctuations in the valve chamber, the peak pressure $P_{v\cdot peak}$, and pressure holding time during lifting operation Δt observed for the different drain pipe angles.

Since the number of water hammer occurrences decreases as the drain pipe angle increases as indicated in Figure 10, the interval of temporal fluctuations in pressure in the valve chamber is longer at larger drain pipe angles, as seen in Figure 11.

At the largest drain pipe angle θ_d= 90[°], gravity acts in the direction opposite to the closing of the drain valve and the loss due to the curvature of the drain pipe is large. Thus, the closing operation of the drain valve is less responsive and the peak of pressure increase due to the occurrence of water hammer is somewhat smaller compared to when the drain pipe angle is θ_d = 0[°].

It was also found that the pressure holding time during lifting operation Δt remains almost invariant regardless of the drain pipe angle.

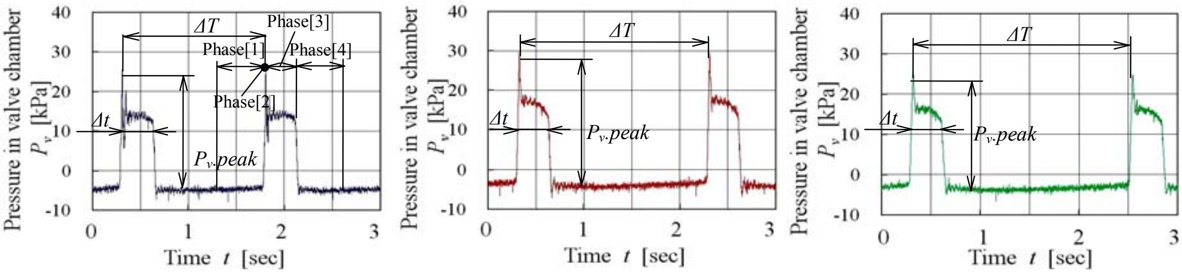

(a) θ_d=0[°] (b) θ_d=45[°] (c) θ_d=90[°]

Fig. 11 Pressure fluctuations due to drain pipe angle (spring length ℓ_s = 46.7 [mm])

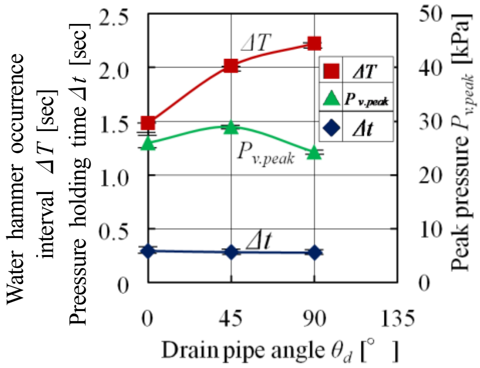

Fig. 12 Relationship between pressure holding time Δt, water hammer occurrence interval ΔT and drain pipe angle

4. Conclusions

This study experimentally examined how the length of a spring attached to the drain valve and the drain pipe angle, which are major components of the water hammer pump among other form factors around the drain valve, affect the performance of the water hammer pump. It produced the following findings.

(1) The pump head vs. flow rate characteristics at varying spring lengths are represented by downward-sloping curves and the curves are at higher flow rate side at lower pump heads as spring length decreases, but performance curves are substantially the same for the 2/3- and 1/3-springs. It has also been found that the basic operation of the water hammer pump repeats the operations in Phase 1 to 4 by visualization of flow around the valve chamber.

(2) The basic behavior of temporal fluctuations in pressure in the valve chamber is substantially the same regardless of spring length, whereas the number of water hammer occurrences increases as the spring length decreases. The peak pressure $P_{v\cdot peak}$ in the valve chamber is larger at higher pump heads. The pressure holding time during lifting operation Δt is larger at smaller pump heads and tends to slightly increase as the spring length increases.

(3) At drain pipe angle $\theta_d = 0$[°], the pump head vs. flow rate characteristics are represented by downward-sloping curves, but the operation range is extremely narrow at larger drain pipe angles. This is due to the effect of gravity acting in the opening direction of the drain valve and the decrease in water hammer occurrence caused by the increase in the drain pipe angle.

Nomenclature

C	Number of water hammer occurrences [count/min]	Q_u	Lifted flow rate [L/min]
D	Drive pipe inner diameter [mmφ]	ΔT	Water hammer occurrence interval [s]
D	Lift pipe inner diameter [mmφ]	Δt	Pressure holding time during lifting operation [s]
H	Water level [m]	V	Air chamber capacity [L]
H	Pump head [m]	V_a	Air volume in the air chamber [L]
L	Drive pipe length [m]	Θ	Drive pipe angle [°]
ℓ_s	Spring length [mm]	θ_d	Drain pipe angle [°]
P_v	Pressure in the valve chamber [kPa]	H	Pump efficiency (see Equation (1).) [%]
Q_d	Drain flow rate [L/min]	η_v	Volumetric efficiency (see Equation (1).) [%]
Q_i	Input flow rate [L/min]	*peak*	Peak pressure (subscript)

References

[1] Kagami, K., Ide, T., and Ushiyama, I., 2001, “Water hammer pump production handboo,” (in Japanese), POWERSHA Inc., pp. 47.

[2] Yunoki, T., 2004, “Production of a Hydraulic Ram Pump and its Research on its Characteristic,” Japan Society for Science Education, (in Japanese), Vol. 28, No .2, pp. 94-100.

[3] Tessema, A. A., 2000, “Hydraulic Ram Pump System Design and Application,” Proceedings of ESME 5th Annual Conference on Manufacturing and Process Industry, September 2000, pp. 1-8.

[4] Hasegawa, S., Suehiro, H., and Yamaguchi, K., 1984, “Trial of Hydraulic Ram and Its Performance Characteristics,” Research Reports of Toyota College of Technology, (in Japanese), No. 17, pp. 15-20.

[5] Taye, T., 1998, “Hydraulic Ram Pump,” Journal of the ESME, Vol. II, No. 1 (1998-7), pp. 1-11.

[6] Okada, U., Uetsuki, H., and Takenaka, T., 1982, “Research on Water Hammer Pump (1st Rep. Mathematical Model on Water Hammer Pump), Turbomachinery, (in Japanese), Vol. 10, No. 6 (1982-6), pp. 323-334.

[7] Saito, S., Nagata, Y., Takahashi, M., Inoue, D., and Hoshino, Y., “Relationship between the Basic Geometric Form and Hydraulic Characteristics of Water Hammer Pump,” Transactions of the Japan Society of Mechanical Engineers, Series B, No. 09-1092, (in Japanese), Vol. 76, No. 767 (2010-7), pp. 1028-1034.

[8] Saito, S., Takahashi, M., and Nagata, Y., “Effects of the Air Volume in the Air Chamber on the Performance of Water Hammer Pump System,” Turbomachinery, (in Japanese), Vol. 39, No. 2 (2011-2), pp.87-94.